Empirical Constraints on the Nucleosynthesis of Nitrogen

James W. Johnson,[1]★ David H. Weinberg,[1,2,3] Fiorenzo Vincenzo,[1,2] Jonathan C. Bird,[4] and and Emily J. Griffith[1]

[1] *Department of Astronomy, The Ohio State University, 140 W. 18th Ave., Columbus, OH, 43210, USA*
[2] *Center for Cosmology and Astroparticle Physics (CCAPP), The Ohio State University, 191 W. Woodruff Ave., Columbus, OH, 43210, USA*
[3] *Institute for Advanced Study, 1 Einstein Dr., Princeton, NJ, 08540, USA*
[4] *Department of Physics & Astronomy, Vanderbilt University, 2301 Vanderbilt Place, Nashville, TN, 37235, USA*

Accepted XXX; Received YYY; in original form ZZZ

ABSTRACT

We use a multi-ring galactic chemical evolution model to probe the astrophysical production of nitrogen (N) in the Milky Way. This approach treats individual annuli in the Galaxy disc as conventional one-zone models, and to include the effects of radial migration, stellar populations move between annuli in a manner based on star particles from a hydrodynamical simulation. We find that some recent AGB star yield tables are able to reproduce the gas-phase [N/O]-[O/H] relation as observed only if a substantial fraction of massive stars collapse to black holes. If instead most massive stars explode as supernovae, we must artificially increase N yields from AGB stars by factors of $2 - 3$ to offset the additional oxygen. We demonstrate that, with a viable set of AGB star yields, our model is able to reproduce many of the observed correlations between N, O, and Fe abundances for stars when the N abundances are corrected for internal mixing processes within stars. With any of these yields, N production timescales are sufficiently short such that stellar migration is only a minimal source of intrinsic scatter in the observed [N/O]-[O/H] relation. Modest variations in the star formation rate and star formation efficiency produce considerably larger variations in the gas phase N and O abundances, consistent with previous observational arguments. Our models run using the publicly available `Versatile Integrator for Chemical Evolution` (`VICE`; `https://pypi.org/project/vice`).

Key words: methods: numerical – galaxies: abundances, evolution, star formation, stellar content

1 INTRODUCTION

From a nucleosynthesis perspective, nitrogen (N) is a unique element. Along with carbon (C) and helium (He), it is one of only three elements produced in asymptotic giant branch (AGB) stars that are lighter than iron peak nuclei (Johnson 2019). N is also a by-product of the nuclear fusion reactions converting hydrogen (H) into He in stars more massive than the sun with nonzero metallicity. The CNO cycle[1] catalyses the proton-proton chain of nuclear reactions (e.g. Suliga, Shalgar & Fuller 2020) using C, N, and oxygen (O) target nuclei. The slowest component of this chain reaction by far is the ^{14}N(p,γ)^{15}O component. As a consequence of this bottleneck, to first order the effect of the CNO cycle is to convert all of the C and O isotopes present in a star's core into ^{14}N. Furthermore, N is among a select group of elements whose observed abundances in stellar spectra often do not reflect the star's birth abundances. Because N is produced in main sequence stars via the CNO cycle, its abundances in a star's core become enhanced relative to what the star was born with. Upon becoming a red giant, internal mixing processes (i.e. dredge-up) bring this N-enhanced material to the photosphere. This phenomenon is both expected from theoretical models and observed in open and globular clusters (Gilroy 1989; Korn et al. 2007; Lind et al. 2008; Souto et al. 2018, 2019; Vincenzo et al. 2021).

Both observationally and theoretically, N is among the more well-studied elements. Of particular interest in this paper is the correlation between the abundances of N and O, usually observed in the gas phase. In Fig. 1, we present a compilation of such measurements:

1. HII regions in the first six CHAOS[2] galaxies (NGC 3184, NGC 628, NGC 5194, NGC 5457, M101, NGC 2403; Berg et al. 2020; Skillman et al. 2020; Rogers et al. 2021).
2. HII regions in nearby NGC spirals (Pilyugin, Vílchez & Thuan 2010).
3. HII regions in blue, diffuse star forming dwarf galaxies (Berg et al. 2012; Izotov, Thuan & Guseva 2012; James et al. 2015).
4. Local stars and HII regions (Dopita et al. 2016).
5. Galactic and extragalactic HII regions (Henry, Edmunds & Köppen 2000).
6. Star-forming regions in 550 nearby galaxies in the MaNGA IFU[3] survey (Belfiore et al. 2017).

Despite intrinsic scatter and some systematic variation in how the

★ Contanct e-mail: johnson.7419@osu.edu
[1] ^{12}C(p, γ)^{13}N(β^+, ν_e)^{13}C(p, γ) ^{14}N(p, γ)^{15}O(β^+, ν_e)^{15}N(p, α) ^{12}C
[2] CHAOS: CHemical Abundances of Spirals (Berg et al. 2015)
[3] MaNGA: Mapping Nearby Galaxies at Apache Point Observatory (Bundy et al. 2015). IFU: Integral Field Unit.

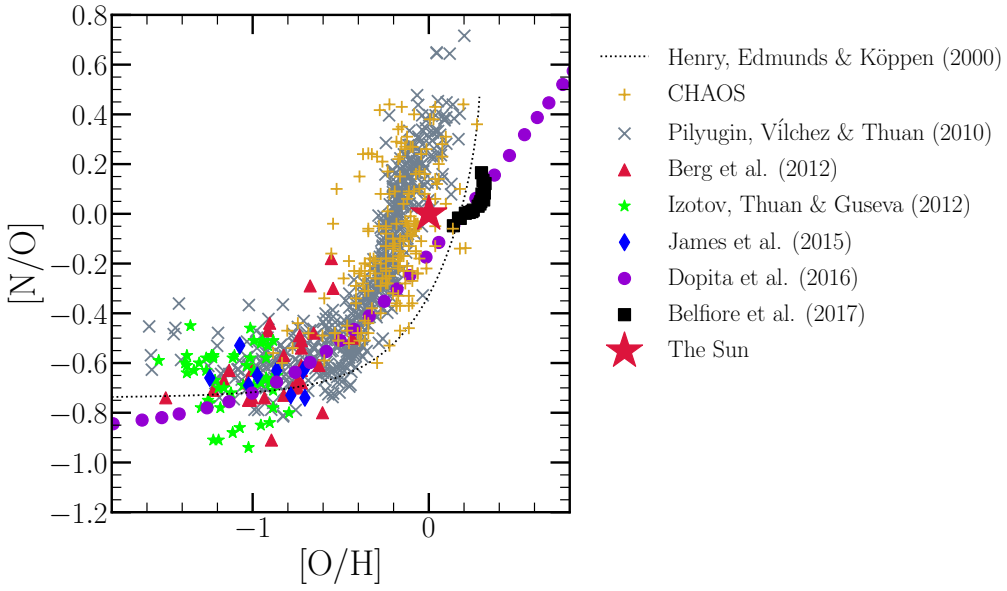

Figure 1. The [N/O]-[O/H] relation as observed in different galactic environments: HII regions from the first six CHAOS galaxies (golden +'s: NGC 3184, NGC 628, NGC 5194, NGC 5457, M101, and NGC 2403; Berg et al. 2020; Skillman et al. 2020; Rogers et al. 2021) and other nearby NGC spiral galaxies (grey X's; Pilyugin et al. 2010), HII regions in blue diffuse star forming dwarf galaxies (red triangles: Berg et al. 2012; green stars: Izotov et al. 2012; blue diamonds: James et al. 2015), in local stars and HII regions (purple circles: Dopita et al. 2016), and in the MaNGA IFU survey (black squares: Belfiore et al. 2017). The fit to [N/O] as a function of [O/H] in Galactic and extragalactic HII regions by Henry et al. (2000) is shown in a black dotted line. We omit all uncertainties for visual clarity. The Sun, at (0, 0) on this plot by definition, is marked by a large red star.

abundances are determined, this [N/O]-[O/H][4] relation is more or less the same across a wide range of astrophysical environments. Here we are interested in the origin of both the shape and scatter in this trend.

N is not unique in that perhaps the largest source of uncertainty in understanding its abundances is that accurate and precise nucleosynthetic yields from various enrichment channels remain elusive. Presently, no combination of models for nucleosynthesis in and explosions of massive stars is able to reproduce the observed abundance pattern of the elements, and N is no exception (Griffith et al. 2021). Recently, Grisoni, Matteucci & Romano (2021) argued that rotating massive stars play a key role in establishing the N abundances seen in metal-poor stars in the Milky Way. Rotation has a considerable impact on the N yields of massive stars, because the internal mixing that it causes (Zahn 1992; Maeder & Zahn 1998; Lagarde et al. 2012) brings internally produced C and O nuclei into the H-burning shell where they can be processed into ^{14}N via the CNO cycle (Heger & Woosley 2010; Frischknecht et al. 2016; Andrews et al. 2017). We find similar results here comparing various theoretical models for massive star nucleosynthesis (see discussion in § 2.1).

Theoretical models for AGB star nucleosynthesis predict N yields to vary as a function of progenitor mass and metallicity (Cristallo et al. 2011, 2015; Karakas 2010; Karakas & Lugaro 2016; Karakas et al. 2018; Ventura et al. 2013, 2014, 2018, 2020). In sufficiently massive AGB stars, the base of the convective envelope is hot enough to activate proton capture reactions, allowing the CNO cycle to convert C and O isotopes in ^{14}N: a process known as hot bottom burning (HBB). AGB stars are also known to experience thermal pulsations, and with each pulse the convective envelope penetrates into the CO-rich core, bringing some of this material into the envelope: a process known as third dredge-up (TDU)[5]. When both processes are active, each TDU episode adds new seed nuclei for HBB to turn into ^{14}N, substantially increasing the N yields. We demonstrate in §§ 2.2 and 2.3 that various theoretical models predict significantly different N yields for high mass AGB stars as a consequence of how TDU and HBB occur in the models. The differences in these processes are in turn a consequence of the microphysical assumptions built into the stellar evolution models (e.g. mass loss, opacity, convection and convective boundaries, nuclear reaction networks).

In this paper, we aim to constrain N yields from AGB stars empirically by assessing to what extent various "off-the-shelf" yield models are able to reproduce the observed correlations between N, O, and iron (Fe), such as the [N/O]-[O/H] relation illustrated in Fig. 1. Vincenzo et al. (2021) demonstrate that when N abundances are corrected for internal mixing processes, the correlations with stellar age and other elemental abundances are affected. Whether or not our galactic chemical evolution (GCE) model is able to reproduce their corrected data constitutes a valuable test not only of our understanding of N nucleosynthesis, but also the accuracy of the Vincenzo et al. (2021) measurements which take a model-dependent approach to estimate the birth abundances of N for a sample of stars.

We make use the multi-zone chemical evolution model for the Milky Way published in Johnson et al. (2021), which treats the Galaxy as a series of concentric rings and tracks the enrichment rates within each ring. This approach has been employed in the past to compute abundances for many Galactic regions (Matteucci & Francois 1989; Wyse & Silk 1989; Prantzos & Aubert 1995; Schönrich & Binney 2009; Minchev, Chiappini & Martig 2013, 2014; Minchev et al.

[4] We follow standard notation where $[X/Y] \equiv \log_{10}(X/Y) - \log_{10}(X/Y)_\odot$.

[5] Here the time adverbial "third" refers only to the fact that these dredge-up episodes are occurring while the star is on the asymptotic giant branch. There is a first TDU, a second TDU, a third TDU, and so on.

2017; Sharma, Hayden & Bland-Hawthorn 2020). A novel aspect of the Johnson et al. (2021) model is that it relaxes the assumption that stars only enrich the Galactic region they were born in by tracking enrichment rates as stellar populations migrate. Originally developed to study the abundances of O and iron (Fe), this aspect of Galactic evolution turned out to have an important impact on the delayed type Ia supernova (SN Ia) enrichment of Fe. Here we use similar methodology to test for similar effects in the delayed AGB star production of N.

In a sample of 6,507 galaxies from the MaNGA IFU survey (Bundy et al. 2015), Schaefer et al. (2020) demonstrated that the intrinsic scatter in the [N/O]-[O/H] relation at fixed galaxy mass is correlated with variations in the local star formation efficiency (SFE). In regions of slower star formation, [N/O] tends to be slightly higher at fixed [O/H] (see their Fig. 4). This is expected from GCE models, because more AGB stars will enrich the ISM with N by the time a given [O/H] is reached (e.g. Mollá et al. 2006; Vincenzo et al. 2016a). However, Schaefer et al. (2020) did not rule out stellar migration as an additional source of scatter in the gas phase [N/O]-[O/H] relation. In principle, there could be a deficit or surplus of N-producing AGB stars in a given Galactic region at any time simply because the orbits are evolving, and this could drive additional scatter in the correlation. This is the same effect as Johnson et al. (2021) found for SNe Ia, but applied to a different enrichment channel. By using the Johnson et al. (2021) model to take into account the effects of migration, we aim to assess whether one of stellar migration or variability in the local SFE are the dominant sources of this scatter.

2 NUCLEOSYNTHESIS

In this paper we make use of the chemical evolution model for the Milky Way presented in Johnson et al. (2021). This model runs using the publicly available `Versatile Integrator for Chemical Evolution` (`VICE`; Johnson & Weinberg 2020; Griffith et al. 2021; Johnson et al. 2021), an open-source `PYTHON` package designed for GCE modeling. Johnson et al. (2021) focus their discussion of the model predictions on O and Fe, and we retain their yields of these elements here. As required by `VICE`, the SN yields are defined as the net mass of some element X produced over all explosion events in units of the progenitor cluster's mass. For example, with a yield of $y_X = 0.001$, a hypothetical $1000 M_\odot$ star cluster would produce $1 M_\odot$ of the element X instantaneously in the case of core collapse supernovae (CCSNe) or over the delay-time distribution (DTD) in the case of SNe Ia. We adopt the following values from Johnson et al. (2021), who in turn base them off of Weinberg, Andrews & Freudenburg (2017) and Johnson & Weinberg (2020):

- $y_O^{CC} = 0.015$
- $y_{Fe}^{CC} = 0.0012$
- $y_O^{Ia} = 0$
- $y_{Fe}^{Ia} = 0.00214$

We also assume that N is not produced in significant amounts by SNe Ia (Johnson 2019), and set y_N^{Ia} throughout this paper accordingly. We spend the remainder of this section detailing our CCSN and AGB star yields of N.

2.1 Core Collapse Supernovae and Massive Star Winds

In `VICE`, CCSN nucleosynthetic products are approximated to be produced instantaneously following an episode of star formation; this is a valid approximation due to how short the lives of massive stars are compared to the relevant timescales for GCE. Based on this and its definition as being in units of a stellar population's total mass, the yield is simply the constant of proportionality between the CCSN production rate and the star formation rate (SFR):

$$\dot{M}_X^{CC} = y_X^{CC} \dot{M}_\star \tag{1}$$

More generally, y_X^{CC} quantifies *all* of the nucleosynthetic material approximated to be produced instantaneously following a single stellar population's formation, though the majority of such events for which this approximation is valid will be associated with massive stars and/or their supernovae. In the case of N specifically, a substantial amount emerges in winds before the actual supernova itself, allowing massive stars to produce a lot N even if they collapse directly to a black hole (Griffith et al. 2021).

We compute theoretically predicted values of y_N^{CC} using `VICE`'s `vice.yields.ccsne.fractional` function assuming a Kroupa (2001) IMF; details on how `VICE` handles these calculations can be found in § 4 of Griffith et al. (2021) and in the `VICE` science documentation[1]. In the left panel of Fig. 2, we plot the results as a function of progenitor metallicity as predicted by the Woosley & Weaver (1995), Nomoto, Kobayashi & Tominaga (2013), Sukhbold et al. (2016), and Limongi & Chieffi (2018) tables. There is good agreement between the various non-rotating models, but only Limongi & Chieffi (2018) report yields for progenitors with non-zero rotational velocities; these yields are substantially larger than that of their non-rotating counterparts. Most of the N production in CCSN progenitors occurs via the CNO cycle processing C and O isotopes into ^{14}N, and with few C and O seed nuclei at low Z, production of ^{14}N is difficult. Rotation-induced mixing, a highly uncertain process (Zahn 1992; Maeder & Zahn 1998; Lagarde et al. 2012), could transport newly produced C and O into the hydrogen burning shell of the CCSN progenitor, facilitating ^{14}N production (Frischknecht et al. 2016; see also discussion in § 4.2 of Andrews et al. 2017). For this reason, N yields at low metallicity are quite sensitive to these assumptions about stellar rotation and internal mixing processes (Heger & Woosley 2010), and consequently IMF-averaged yields are highly uncertain.

Based on the definition of the abundance ratio [X/Y], we can compute the [N/O] ratio of CCSN ejecta from the values of y_N^{CC} and y_O^{CC} predicted from a given yield table:

$$[\mathrm{N/O}]_{cc} = \log_{10}\left(\frac{y_N^{CC}}{y_O^{CC}}\right) - \log_{10}\left(\frac{Z_{N,\odot}}{Z_{O,\odot}}\right), \tag{2}$$

where $Z_{X,\odot}$ is the abundance by mass of some element X in the sun, for which we take $Z_{N,\odot} = 6.91 \times 10^{-4}$ and $Z_{O,\odot} = 5.72 \times 10^{-3}$ based on the solar photospheric abundances of Asplund et al. (2009). For each of the published yield tables and rotational velocities in the left panel of Fig. 2, we compute the corresponding values of y_O^{CC} using `VICE`and plot the resultant values of $[\mathrm{N/O}]_{cc}$ in the right panel. These yield ratios follow similar trends with progenitor metallicity and rotation as y_N^{CC} itself, a consequence of the fact that these studies predict relatively metallicity-independent O yields.

CCSN yields can to some extent be empirically calibrated by ensuring that they reproduce the [N/O] ratios of low metallicity systems. Since AGB star yields of N are believed to depend on the progenitor's metallicity (see discussion in § 2.2 and references

[1] `https://vice-astro.readthedocs.io/en/latest/science_documentation/yields`

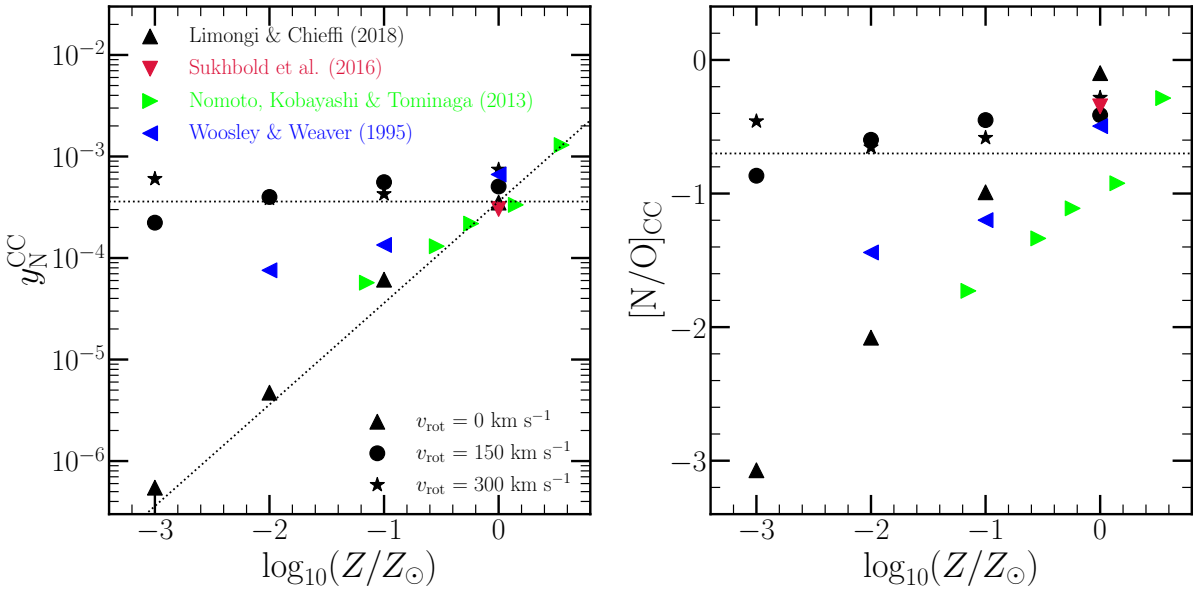

Figure 2. Left: IMF-averaged CCSN yields of N calculated using `VICE`'s `vice.yields.ccsne.fractional` function with the tables published by Woosley & Weaver (1995, blue), Nomoto et al. (2013, green), Sukhbold et al. (2016, red), and Limongi & Chieffi (2018, black). All studies report yields for non-rotating progenitors, shown by the triangles; for visual clarity, the triangles point in a different direction for each study according to the legend. Limongi & Chieffi (2018) report additional yields for progenitors with rotational velocities of 150 (circles) and 300 km/s (stars). The horizontal dashed line marks $y_{\rm N}^{\rm CC} = 3.6 \times 10^{-4}$, the value of our fiducial CCSN yield of N in our GCE models. We use the form shown by the slanted line (equation X) in § X in combination with some of our AGB star yield models discussed in § 2.2. **Right**: The [N/O] ratio predicted by each of the explosion models in the left-hand panel, under the same colour-coding and marker scheme. We mark the position of [N/O] = −0.7 with a black dotted line, the value roughly suggested by the observations of low-metallicity systems highlighted in Fig. 1.

therein), it's likely that the "plateau" in [N/O] at low [O/H] reflects the IMF-averaged CCSN yields of N and O. Fig. 1 suggests that $[{\rm N/O}]_{\rm cc} = -0.7$; we highlight this value in the right panel of Fig. 2 with a horizontal black dashed line. Given this observational result and our adopted value of $y_{\rm O}^{\rm CC} = 0.015$, we compute that an empirical N yield of $y_{\rm N}^{\rm CC} = 3.6 \times 10^{-4}$ using equation (2). We adopt this value as our fiducial CCSN yield of N and highlight it with a horizontal black dashed line in the left panel of Fig. 2. We discuss the sloped dotted line in that panel in the context of some of our AGB star yield models in § X.

These empirical values of $[{\rm N/O}]_{\rm cc}$ and $y_{\rm N}^{\rm CC}$ are in good agreement with the rotating CCSN models of Limongi & Chieffi (2018). This supports the recent argument by Grisoni et al. (2021) that rotating massive stars play an important role in establishing the N abundances observed at low metallicities in the Milky Way. Although the Sukhbold et al. (2016) tables agree nearly perfectly with our empirical value of $y_{\rm N}^{\rm CC} = 3.6 \times 10^{-4}$, they overestimate $[{\rm N/O}]_{\rm cc}$ by ∼0.2 dex; this is because they predict a value of $y_{\rm O}^{\rm CC}$ lower than our adopted value of 0.015. Although most of the supernova models plotted in Fig. 2 slightly overestimate our empirical value of $[{\rm N/O}]_{\rm cc} = -0.7$, they still fall short of solar. This implies the need for an additional enrichment, which is expected because it is well understood that N is also produced in considerable amounts by AGB stars (Johnson 2019).

2.2 Asymptotic Giant Branch Stars

2.3 IMF-Averaged AGB Star Yields: Metallicity and Time Dependence

3 ACKNOWLEDGEMENTS

We are grateful to Amanda Karakas for valuable discussion on the physical processes affecting N production in asymptotic giant branch stars. We thank Paolo Ventura for providing asymptotic giant branch star yields at a wide variety of progenitor metallicities. We acknowledge valuable discussion with Jennifer Johnson, Adam Leroy, Grace Olivier, Amy Sardone, Jiayi Sun, Todd Thompson, and other members of The Ohio State Astronomy Gas, Galaxies, and Feedback group. This work was supported by National Science Foundation grant AST-1909841. D.H.W. is grateful for the hospitality of the Institute for Advanced Study and the support of the W.M. Keck Foundation and the Hendricks Foundation. F.V. acknowledges the support of a Fellowship from the Center for Cosmology and Astroparticle Physics at The Ohio State University.

REFERENCES

Andrews B. H., Weinberg D. H., Schönrich R., Johnson J. A., 2017, ApJ, 835, 224
Asplund M., Grevesse N., Sauval A. J., Scott P., 2009, ARA&A, 47, 481
Belfiore F., et al., 2017, MNRAS, 469, 151
Berg D. A., et al., 2012, ApJ, 754, 98
Berg D. A., Skillman E. D., Croxall K. V., Pogge R. W., Moustakas J., Johnson-Groh M., 2015, ApJ, 806, 16
Berg D. A., Pogge R. W., Skillman E. D., Croxall K. V., Moustakas J., Rogers N. S. J., Sun J., 2020, ApJ, 893, 96
Bundy K., et al., 2015, ApJ, 798, 7

Cristallo S., et al., 2011, ApJS, 197, 17
Cristallo S., Straniero O., Piersanti L., Gobrecht D., 2015, ApJS, 219, 40
Dopita M. A., Kewley L. J., Sutherland R. S., Nicholls D. C., 2016, Ap&SS, 361, 61
Frischknecht U., et al., 2016, MNRAS, 456, 1803
Gilroy K. K., 1989, ApJ, 347, 835
Griffith E. J., Sukhbold T., Weinberg D. H., Johnson J. A., Johnson J. W., Vincenzo F., 2021, arXiv e-prints, p. arXiv:2103.09837
Grisoni V., Matteucci F., Romano D., 2021, arXiv e-prints, p. arXiv:2109.03642
Gronow S., Cote B., Lach F., Seitenzahl I. R., Collins C. E., Sim S. A., Roepke F. K., 2021a, arXiv e-prints, p. arXiv:2103.14050
Gronow S., Collins C. E., Sim S. A., Röpke F. K., 2021b, A&A, 649, A155
Heger A., Woosley S. E., 2010, ApJ, 724, 341
Henry R. B. C., Edmunds M. G., Köppen J., 2000, ApJ, 541, 660
Hurley J. R., Pols O. R., Tout C. A., 2000, MNRAS, 315, 543
Izotov Y. I., Thuan T. X., Guseva N. G., 2012, A&A, 546, A122
James B. L., Koposov S., Stark D. P., Belokurov V., Pettini M., Olszewski E. W., 2015, MNRAS, 448, 2687
Johnson J. A., 2019, Science, 363, 474
Johnson J. W., Weinberg D. H., 2020, MNRAS, 498, 1364
Johnson J. W., et al., 2021, arXiv e-prints, p. arXiv:2103.09838
Karakas A. I., 2010, MNRAS, 403, 1413
Karakas A. I., Lugaro M., 2016, ApJ, 825, 26
Karakas A. I., Lugaro M., Carlos M., Cseh B., Kamath D., García-Hernández D. A., 2018, MNRAS, 477, 421
Kodama T., Arimoto N., 1997, A&A, 320, 41
Korn A. J., Grundahl F., Richard O., Mashonkina L., Barklem P. S., Collet R., Gustafsson B., Piskunov N., 2007, ApJ, 671, 402
Kroupa P., 2001, MNRAS, 322, 231
Lagarde N., Decressin T., Charbonnel C., Eggenberger P., Ekström S., Palacios A., 2012, A&A, 543, A108
Larson R. B., 1974, MNRAS, 166, 585
Limongi M., Chieffi A., 2018, ApJS, 237, 13
Lind K., Korn A. J., Barklem P. S., Grundahl F., 2008, A&A, 490, 777
Maeder A., Meynet G., 1989, A&A, 210, 155
Maeder A., Zahn J.-P., 1998, A&A, 334, 1000
Matteucci F., Francois P., 1989, MNRAS, 239, 885
Minchev I., Chiappini C., Martig M., 2013, A&A, 558, A9
Minchev I., Chiappini C., Martig M., 2014, A&A, 572, A92
Minchev I., Steinmetz M., Chiappini C., Martig M., Anders F., Matijevic G., de Jong R. S., 2017, ApJ, 834, 27
Mollá M., Vílchez J. M., Gavilán M., Díaz A. I., 2006, MNRAS, 372, 1069
Nomoto K., Kobayashi C., Tominaga N., 2013, ARA&A, 51, 457
Padovani P., Matteucci F., 1993, ApJ, 416, 26
Pilyugin L. S., Vílchez J. M., Thuan T. X., 2010, ApJ, 720, 1738
Prantzos N., Aubert O., 1995, A&A, 302, 69
Rogers N. S. J., Skillman E. D., Pogge R. W., Berg D. A., Moustakas J., Croxall K. V., Sun J., 2021, ApJ, 915, 21
Schaefer A. L., Tremonti C., Belfiore F., Pace Z., Bershady M. A., Andrews B. H., Drory N., 2020, ApJ, 890, L3
Schönrich R., Binney J., 2009, MNRAS, 396, 203
Sharma S., Hayden M. R., Bland-Hawthorn J., 2020, arXiv e-prints, p. arXiv:2005.03646
Skillman E. D., Berg D. A., Pogge R. W., Moustakas J., Rogers N. S. J., Croxall K. V., 2020, ApJ, 894, 138
Souto D., et al., 2018, ApJ, 857, 14
Souto D., et al., 2019, ApJ, 874, 97
Sukhbold T., Ertl T., Woosley S. E., Brown J. M., Janka H. T., 2016, ApJ, 821, 38
Suliga A. M., Shalgar S., Fuller G. M., 2020, arXiv e-prints, p. arXiv:2012.11620
Ventura P., Di Criscienzo M., Carini R., D'Antona F., 2013, MNRAS, 431, 3642
Ventura P., di Criscienzo M., D'Antona F., Vesperini E., Tailo M., Dell'Agli F., D'Ercole A., 2014, MNRAS, 437, 3274
Ventura P., Karakas A., Dell'Agli F., García-Hernández D. A., Guzman-Ramirez L., 2018, MNRAS, 475, 2282
Ventura P., Dell'Agli F., Lugaro M., Romano D., Tailo M., Yagüe A., 2020, A&A, 641, A103
Vincenzo F., Belfiore F., Maiolino R., Matteucci F., Ventura P., 2016a, MNRAS, 458, 3466
Vincenzo F., Matteucci F., de Boer T. J. L., Cignoni M., Tosi M., 2016b, MNRAS, 460, 2238
Vincenzo F., et al., 2021, arXiv e-prints, p. arXiv:2106.03912
Weinberg D. H., Andrews B. H., Freudenburg J., 2017, ApJ, 837, 183
Woosley S. E., Weaver T. A., 1995, ApJS, 101, 181
Wyse R. F. G., Silk J., 1989, ApJ, 339, 700
Zahn J. P., 1992, A&A, 265, 115

Appendices

A VICE

VICE[1] is an open-source PYTHON package designed to model chemical enrichment processes in galaxies with a generic, flexible model. With this paper, we mark the release of version 1.3.0 which presents a handful of new features:

(i) Users may select a mass-lifetime relation for stars from a list of several parameterized forms taken from the literature. Previously, only a single power-law was implemented, but this formulation underestimates lifetimes for stars with masses $\gtrsim 4 M_\odot$; now, the options include the equations presented in:

- Vincenzo et al. (2016b)
- Hurley, Pols & Tout (2000)
- Kodama & Arimoto (1997)
- Padovani & Matteucci (1993)
- Maeder & Meynet (1989)
- Larson (1974) **(default)**

Generally, chemical evolution models make similar predictions with each of these different forms of the mass-lifetime relation since their quantitative predictions are not considerably different from one another (see the section titled "Single Stellar Populations" under VICE's science documentation for further discussion[2]). We select the Larson (1974) form as a default within VICE because it is typical compared to the others and requires the lowest amount of computational overhead (aside from the single power-law option).

(ii) We have added two additional tables of AGB star yields sampled at various progenitor masses and metallicities: the KL16+K18 and V13 models presented in this paper are new to VICE (see discussion in § 2.2 for details).

(iii) We have built in the SN Ia yields presented in Gronow et al. (2021b,a). These tables present yields for double detonations of sub-Chandrasekhar mass carbon-oxygen white dwarfs at various progenitor metallicities.

Although VICE includes built in SN and AGB star yield tables, users are not required to adopt any one of them for use in their chemical evolution models. Instead, it allows arbitrary functions of metallicity for both CCSN and SN Ia yields and functions of progenitor mass and metallicity for AGB star yields. It provides similar flexibility for additional parameters typically built into GCE models. VICE's backend

[1] Install (PyPI): https://pypi.org/project/vice
Documentation: https://vice-astro.readthedocs.io
Source Code: https://github.com/giganano/VICE.git
[2] https://vice-astro.readthedocs.io/en/latest/science_documentation/

is implemented entirely in ANSI/ISO C, providing it with the powerful computing speeds of a compiled library while retaining such scientific flexibility within the easy-to-use framework of PYTHON.

Requiring a Unix kernel, VICE supports Mac and Linux operating systems; Windows users should install and use VICE entirely within the Windows Subsystem for Linux. On machines with x86_64 hardware, it can be installed in a terminal via `pip install vice`. Users running ARM64 hardware (e.g. Macintosh computers with Apple's new M1 processor) must install VICE by compiling from source, instructions for which can be found in the documentation. After installing, running `vice --docs` and `vice --tutorial` from a Unix terminal will launch a web browser to the documentation and to a jupyter notebook intended to familiarize first time users with VICE's API.